Available online at www.sciencedirect.com
SCIENCE DIRECT®
Journal of Molecular Catalysis A: Chemical 228 (2005) 3–10
JOURNAL OF MOLECULAR CATALYSIS A: CHEMICAL
www.elsevier.com/locate/molcata

The stabilization of supported gold clusters by surface defects

W.T. Wallace, B.K. Min, D.W. Goodman*

Department of Chemistry, Texas A&M University, P.O. Box 30012, College Station, TX 77842-3012, USA

Abstract

The chemical and electronic properties of surfaces to a large extent are controlled by defects. Defects facilitate the adsorption of gases and serve as reactive sites for chemical reactions. Furthermore, surface defects are a key to the nucleation, growth, and stability of metal clusters on metal oxide surfaces. This paper summarizes recent studies to assess the role of defects on Au cluster nucleation, growth, and stability on SiO_2 and mixed TiO_x–SiO_2 thin films. For a SiO_2 thin film, Au clusters sinter at elevated temperatures and pressures; however, introduction of defects on a SiO_2 surface as TiO_x islands or as substitutional Ti dramatically decreases the rate of Au cluster sintering.

1. Introduction

Metal clusters dispersed on planar, oxide supports have been used extensively as model catalysts [1–11]. Detailing the function of supported metal catalysts at the atomic level is a challenge, however, because of the typical temperatures and pressures at which such catalyst are operated and the inherent complexity of the catalyst itself. Metal single crystals have been used as simple model catalysts allowing the utilization of most surface analytical tools. However, single crystals preclude the assessment of important catalyst variables such as cluster size and support–cluster interactions [12,13]. Also, ultrahigh vacuum environments preclude studies of the influence of reactant environments on surface intermediates, composition, and morphology. To more realistically model technical catalysts, simplified planar supported cluster catalysts have been synthesized by nucleating metal clusters onto a thin oxide film grown on a refractory metal substrate [13]. These thin oxide films are structurally and electronically similar to the corresponding bulk oxides, yet are thin enough to permit the use of electron spectroscopic techniques [14]. These thin film model catalysts provide new opportunities for studying the unique properties of oxide-supported clusters. Highlights of these studies are summarized in this article.

One of the most active areas of current activity in surface science is the study of defects. Surface defects play an important role in the properties of bulk materials and surfaces. For instance, the introduction of defects into a crystal can dramatically change its electronic properties. Likewise, defects can alter the adsorption properties of reactant gases on various metal surfaces [15–19]. Yates and coworkers studied the non-dissociative adsorption of dinitrogen on Pt(1 1 1) [15] and found that the presence of monovacancy defect sites formed by Ar^+ sputtering produced an intense IR-active nitrogen adsorption. This contrasts with a defect-free surface where no IRAS signal is apparent. Zubkov et al. studied the dissociation of CO on a stepped Ru surface using IRAS, TPD, and isotopic mixing [18] and showed that two-atom high steps on a Ru(1 0 9) surface are responsible for CO dissociation at 480 K. From these results these authors inferred that the special activity of Ru for Fischer–Tropsch catalysis is due to low-coordinated Ru atoms and/or the steric environment near these sites. In general, step defects play a key role in surface chemistry, as summarized by Yates [16].

Defects can also affect the chemistry of bare metal-oxide surfaces [20–23]. Kolmakov et al. studied the defect-induced adsorption effects of MgO thin films towards NO adsorption using photoelectron spectroscopies and temperature programmed desorption [20]. They found that exposure of NO to both regular and defective (with a large number of point defects) MgO films led to changes in the metastable impact electron spectra. A difference spectrum showed remarkable

* Corresponding author.
E-mail address: goodman@mail.chem.tamu.edu (D.W. Goodman).

1381-1169/$ – see front matter © 2004 Elsevier B.V. All rights reserved.
doi:10.1016/j.molcata.2004.09.085

similarity to the gas phase spectrum of N_2O, leading to the conclusion that NO adsorbs dissociatively on MgO at low temperatures and forms N_2O on the surface. The saturation coverages obtained indicated that, while terrace defects may play a role in the dissociation of NO, the adsorption and dissociation of NO generally occurs at extended defects.

Abad et al. studied the dissociative adsorption of NO on stoichiometric and reduced TiO_2(1 1 0) surfaces [23] and noted that NO generally adsorbs molecularly on both oxidized and reduced TiO_2 at low temperatures. In their room temperature studies, these authors found that there was no interaction between NO and the stoichiometric surface, even under exposures of 500 L. However, on surfaces that had been bombarded with Ar^+ ions, producing Ti^{3+} and Ti^{2+} species, exposure to NO led to an increase in Ti^{4+} XPS intensity with a decrease in the reduced species. This result, combined with AES, led to the conclusion that NO dissociates at the point defects on the surface, thereby filling the oxygen vacancies and releasing N_2 into the gas phase.

Defects on metal-oxide supports also play an essential role as metal cluster nucleation sites. For example, for small, size-selected clusters, Heiz and coworkers have reported that oxygen vacancies (point defects) on MgO are essential for the nucleation of active Au clusters [24,25]. Furthermore, theoretical studies have shown that electron transfer from defects to the cluster facilitate CO oxidation. Also, Heiz and Pacchioni, in studies of acetylene polymerization on Pd, have suggested that trapped electrons at oxygen vacancies more efficiently activate single Pd atoms for reaction than do low-coordinated oxygen atoms [26]. Several reviews discussing oxygen vacancies summarize recent relevant theoretical studies related to the metal cluster–oxide interface [27–29].

With respect to the ability of oxide supported metal clusters to act as heterogeneous catalysts, the activity and selectivity of metal-catalyzed reactions are often sensitive to the metal particle morphology. For example, the catalytic activity of Au supported on certain oxides depends critically on the morphology of the clusters [30]. In general, the morphology of metal particles on oxide surfaces depends to a large extent on defects, particularly point defects such as oxygen vacancies [27,31–35] Several studies have addressed the relationship between metal cluster nucleation/growth on oxide surfaces and defects; however, many questions remain unanswered. Most recently, a study by Besenbacher and coworkers using STM showed that bridging oxygen vacancies on TiO_2 are active nucleation sites for Au clusters [31]. In addition, these authors suggested that the diffusion of an oxygen vacancy complex plays an important role in the formation of larger Au clusters. Using AFM, Barth and coworkers have quantified point defects on MgO by estimating the Pd cluster density as a function of the deposition surface temperature [35]. In a theoretical study, Bogicevic and Jennison have calculated the binding energies of various metals to MgO and showed that dimers of noble metals are more stable at oxygen vacancies [27]. Using STM, Freund and coworkers have demonstrated preferential decoration of Pd and Rh metal particles on line defects of Al_2O_3 [33,34]. Very recently, defects on crystalline SiO_2 thin films have been studied in our laboratory using ultraviolet photoelectron spectroscopy (UPS) and metastable impact electron spectroscopy techniques (MIES) [36,37].

Other defects have also been found to be active cluster nucleation sites, as been reported by several groups [9,11,38–42]. Wiltner et al. studied the growth of copper and vanadium on thin alumina films [39] These authors found that, for these two metals, clusters do not preferentially decorate steps or defects, but instead nucleate at one of two superstructures. The growth of bimetallic Co–Pd clusters on alumina was studied by Freund and coworkers [11] who noted that Pd clusters tend to nucleate at domain boundaries of the alumina film (line defects), while Co clusters nucleate at point defects at room temperature. At higher temperatures, Co nucleates at line defects. When deposited in succession, Pd nucleates only on top of the Co particles, forming a core–shell structure, while, due to a larger metal-support interaction, Co deposited following Pd nucleates both on the Pd clusters and at point defects.

In this review, we discuss recent work in our laboratory that has focused on the nucleation and stability of Au clusters on various oxide supports. It has been found that the controlled introduction of defects on a SiO_2 thin film provides stability for the clusters under high temperatures and pressures, which could very well lead to the development of more efficient and stable nanostructured, technical catalysts.

2. Experimental

All experiments were carried out in an ultrahigh vacuum (UHV) apparatus with a base pressure of 5×10^{-10} Torr, consisting of an elevated pressure reactor and a surface analytical chamber, the details of which are described elsewhere [43]. Briefly, the techniques available include X-ray photoelectron spectroscopy (XPS), Auger electron spectroscopy (AES), low energy electron diffraction (LEED), and scanning tunneling microscopy (STM). Following preparation and characterization in the surface analytical chamber, the sample was transferred in situ into the elevated-pressure reactor whose pressure was measured by a MKS Baratron pressure gauge. Ultrahigh purity (99.999%) oxygen from MG industries and a Mo(1 1 2) crystal, oriented to $<0.25^\circ$ (from Matek, Germany), were used in this study. The Mo(1 1 2) surface was cleaned by oxygen treatment and high temperature annealing (2000 K), and the cleanliness was verified with AES. A thermocouple (W–5% Re/W–26% Re) was used to measure the surface temperature and to calibrate an optical pyrometer (OMEGA OS3700). In the STM measurements, the optical pyrometer was used to measure the temperature.

The initial films used for these studies were SiO_2 thin films, for which the synthesis method has been described in detail [44–48]. In order to achieve a high quality, ordered thin film, a Mo(1 1 2) single crystal was first oxidized in

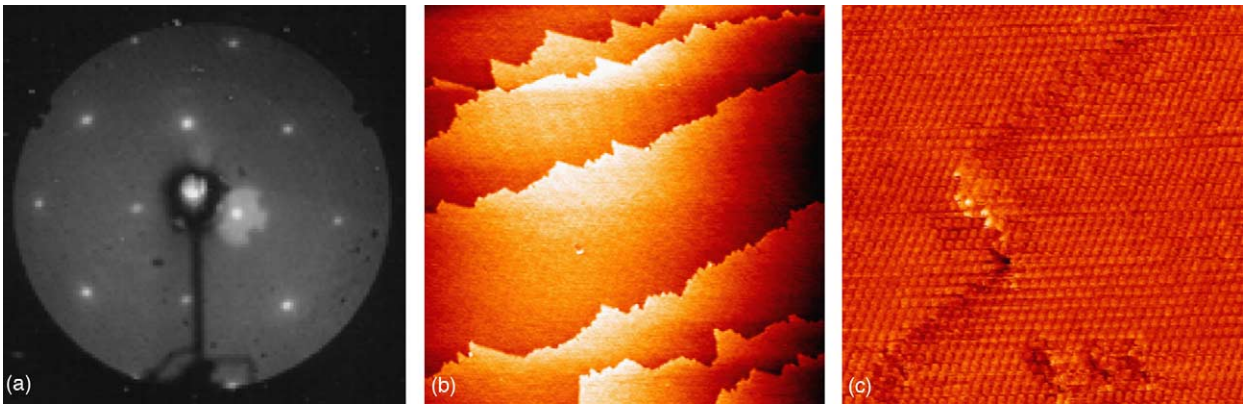

Fig. 1. (a) LEED pattern (E =56 eV) and STM images (U_T = 2.0 V and I = 0.1 nA) of a SiO_2 thin film: (b) 200 nm × 200 nm and (c) 50 nm × 50 nm.

1×10^{-7} Torr O_2 at ∼800 K for 5 min to produce a $p(2 \times 3)$-O structure. The SiO_2 film was prepared sufficiently thick to produce the structural and electronic properties of bulk SiO_2, yet thin enough to allow the use of the full array of surface spectroscopies as well as STM. The Si-covered surface was then oxidized and annealed in O_2 (1×10^{-7} Torr) at ∼1150 K for 30 min. This step forms a highly ordered SiO_2 thin film, as exhibited by a sharp LEED pattern with $c(2 \times 2)$ periodicity and long-range and atomically resolved STM images (Fig. 1(a)–(c)). The formation of a stoichiometric film was confirmed by the absence of Si^0 or Si^{2+} AES features.

In order to produce mixed TiO_x–SiO_2 thin films, a small amount of Ti is deposited onto the crystalline SiO_2 thin film [49]. This is followed by oxidation at 950 K and annealing in vacuum at 1150 K. Depending on the amount of Ti used, different surface morphologies can be obtained. At approximately 8% Ti (in relation to the SiO_2 surface), a surface structure such as that shown in Fig. 2(a) is obtained. As can be seen, compared to the bare silica surface, there are now areas of much brighter contrast. A high-resolution STM image of this surface is shown in Fig. 2(b). The image shows a collection of bright spots corresponding to Ti atoms and less distinct bright areas corresponding to corrugations of the SiO_2 thin film surface. The brightest areas appear along the [1 1 1] direction. The height difference of these bright spots is approximately 0.1 nm, considerably less than the Ti–O bond length, implying that the Ti atoms lie in the plane of the SiO_2 film rather on the surface. In fact, this replacement has already been shown in "real world" mixed titania–silica catalysts [50] Upon further Ti deposition, additional contrast is observed on the step edges and ordered TiO_x structures appear, as shown in Fig. 2(c).

3. Results and discussion

Recently, the nucleation behavior of Au clusters on these thin, crystalline silica films (∼1 ML) [51] has been studied [49]. To date, there has not been a consensus regarding the actual structure of the bare SiO_2 thin films, though several possibilities have been suggested [48,49,52]. Generally, however, three major defects are expected to be present in the films. These are extended defects (steps and kinks), line defects (antiphase domain boundaries), and point defects (oxygen vacancies). From a spot profile analysis LEED study (SPA-LEED) of their SiO_2 thin films, Freund and coworkers sug-

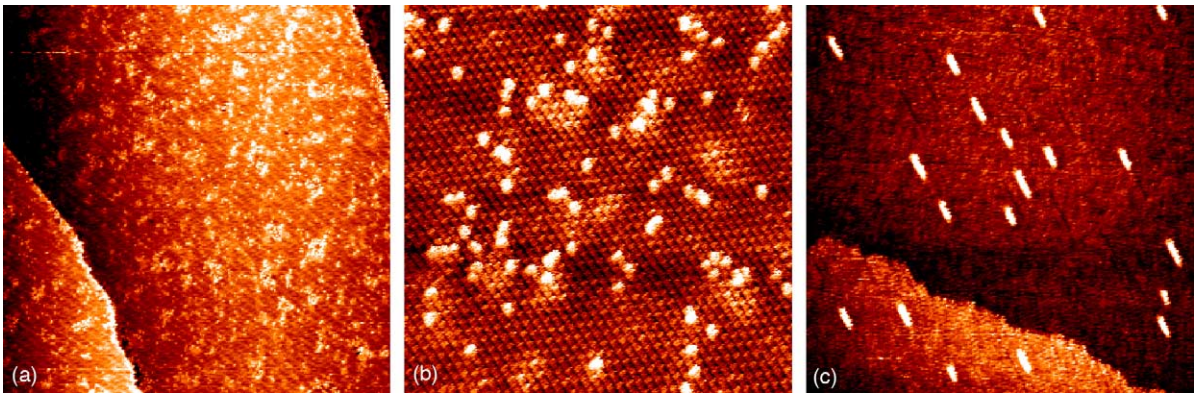

Fig. 2. (a) STM image (200 nm × 200 nm) of a mixed TiO_x–SiO_2 thin film containing approximately 8% Ti; (b) high-resolution STM image of a terrace from the same film (15 nm × 15 nm, U_s = −1.0 V and I = 0.18 nA); (c) STM image (200 nm × 200 nm) of a mixed TiO_x–SiO_2 thin film containing approximately 17% Ti. Ordered TiO_x structures can now be seen on the terraces.

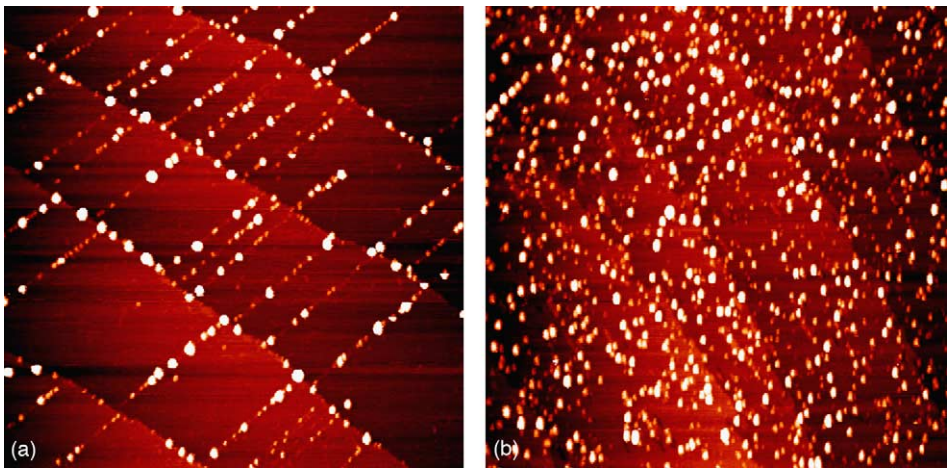

Fig. 3. STM images (200 nm × 200 nm) of Au clusters on (a) a SiO_2 thin film with a small number of point defects and (b) a SiO_2 thin film containing a large number of point defects on the terraces. The gold coverage is approximately 0.4 ML for both images.

gested line defects based on the broadening of the superlattice spots [48]. At room temperature deposition of Au on a film low in point defects, clusters preferentially nucleate and grow on the line defects of the bare SiO_2 thin film. Evidence of this decoration can be seen in the STM image of Fig. 3(a). For a film high in point defects, clusters nucleate and grow at point defects on the terraces, as shown in Fig. 3(b).

Compared to reducible oxide supports, SiO_2 is known to have a relatively weak metal–support interaction with noble metals [53]. Accordingly, sintering due to increased temperatures or pressures is expected to be more pronounced in metal–SiO_2 systems. For gold clusters supported on SiO_2, this is indeed the case, as a thermally induced sintering phenomenon has been observed on the low-defect films. As mentioned above, after room temperature deposition of gold, clusters generally form at the existing line defects of the SiO_2 thin film, but, after annealing at 700 and 850 K, the decoration of line defects is no longer evident. A dramatic decrease in cluster density and an increase in average size accompany the movement of the clusters from the line defects, as shown in Fig. 4. For a highly defective film, however, the cluster density remains relatively high, even at 850 K (Fig. 5) [51].

A dramatic change in the nucleation properties of gold on the silica surface can be produced by the addition of Ti by the methods described above. By substitution into the silica surface, the titania atoms form heterogeneous defects. In turn, gold deposition onto this low-Ti content TiO_x–SiO_2 surface forms clusters with an enhanced number density on terraces and step edges, indicating an increase in nucleation sites. At identical coverages of gold, this effect is evident in Fig. 6 compared to Fig. 3(a). Therefore, it would seem that the Ti "defects" act as nucleation sites for cluster growth. This effect becomes more obvious when a very small amount of gold (0.04 ML) is deposited on the surface. STM images provide a comparison of Ti defects (Fig. 7(a)) and Au clusters nucleated on these defects (Fig. 7(b)). In addition to the bright contrast due to Ti defects, much brighter contrast is observed due to the presence of gold clusters above these defects.

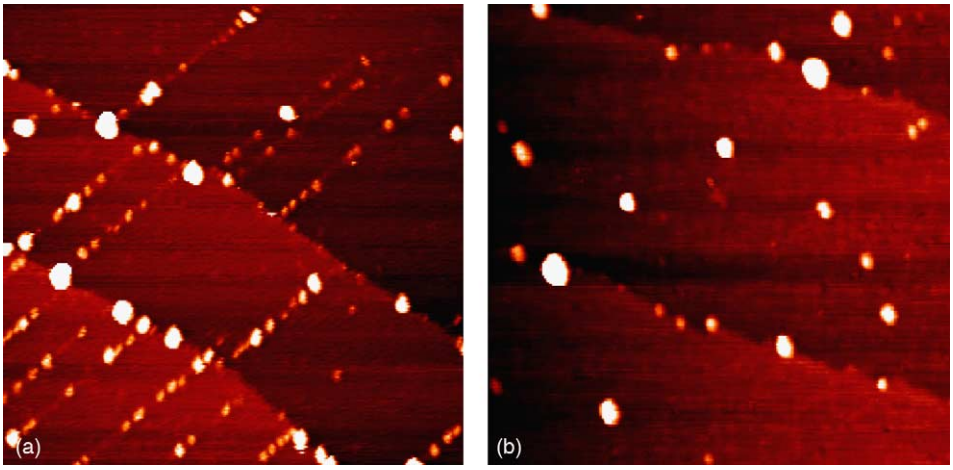

Fig. 4. STM images (200 nm × 200 nm) of 0.4 ML Au on a low-defect SiO_2 thin film (a) before and (b) after annealing to 850 K. Under higher temperatures, the clusters sinter, leading to a loss in cluster number density and an increase in average cluster size.

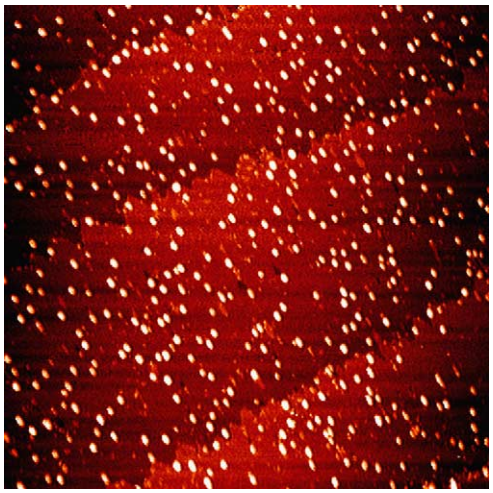

Fig. 5. STM image (200 nm × 200 nm) of 0.4 ML Au on a SiO_2 thin film containing a large number of point defects on the terraces. Upon deposition at 850 K, a high cluster number density is obtained, in contrast to the effects of high temperature seen in Fig. 4.

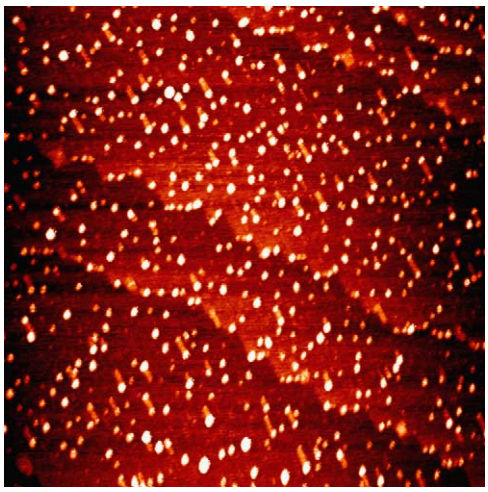

Fig. 6. STM image (200 nm × 200 nm) of 0.4 ML Au deposited on a TiO_x–SiO_2 thin film containing ~17% Ti at room temperature. In contrast to Fig. 3(a), the cluster density is increased dramatically and there is a greater amount of nucleation on the terraces.

Increasing the amount of Ti on the surface eventually leads to saturation of surface sites, at which point TiO_x islands begin to form. These islands also play a role in the nucleation and growth of gold clusters, with nucleation being seen on the edges and/or tops of the rectangular TiO_x islands. These islands with gold clusters are seen in the 3D STM image of Fig. 7(c).

Although the addition of small amounts of Ti (<10%) to the SiO_2 surface leads to an increase in the cluster nucleation probability, it does not affect the tendency for the clusters to

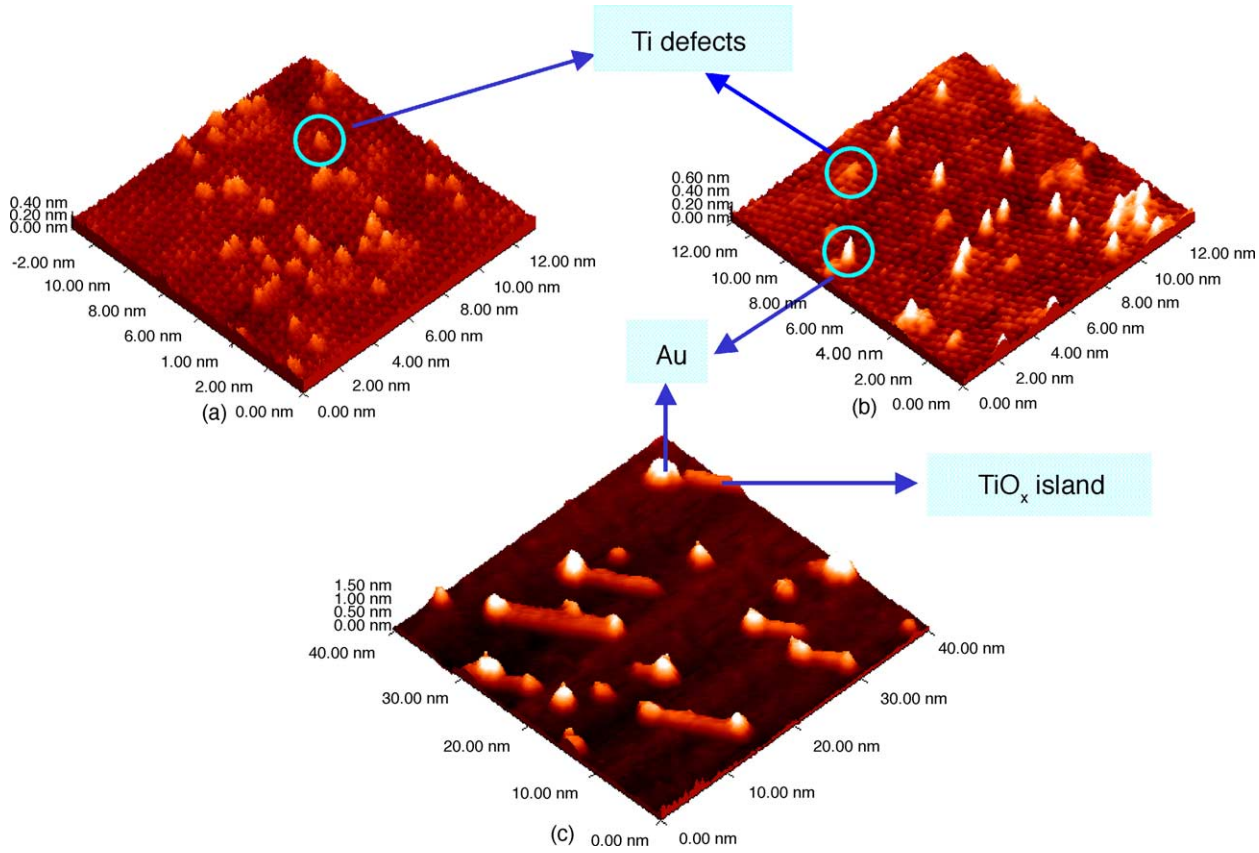

Fig. 7. 3D STM images of (a) TiO_x (8%)–SiO_2; (b) Au (0.04 ML)/TiO_x(8%)–SiO_2; (c) Au (0.08 ML)/TiO_x (17%)–SiO_2 showing that both Ti defects and TiO_x islands play a role as nucleation sites for Au clusters.

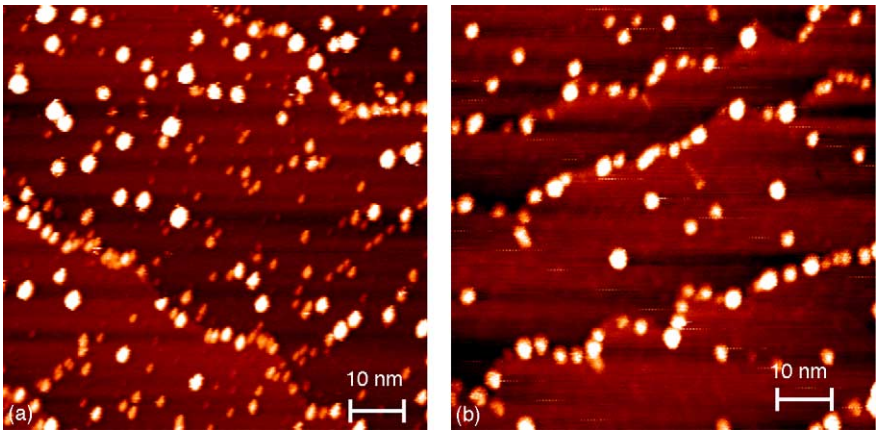

Fig. 8. STM images showing the effects of annealing on Au/TiO_x (8%)–SiO_2: (a) 0.4 ML Au deposited at room temperature; (b) after annealing at 850 K. As with the bare SiO_2 surface, annealing leads to a dramatic decrease in cluster number density and an increase in average cluster size.

sinter under reaction conditions, as is evident in Fig. 8(a) before, and in Fig. 8(b) after, an 850 K anneal. However, sinter resistant properties are observed when the Ti coverage is increased to 17%, showing no apparent morphological change after heating to 850 K (Fig. 9).

Gold clusters supported on TiO_2(1 1 0) are known to be highly active for CO oxidation [8,30]. However, under reaction conditions, the clusters have been found to lose their activity over time. The effects of placing a Au/TiO_2(1 1 0) sample under a 10 Torr CO/O_2 mixture for 2 h can be seen in the STM images of Fig. 10. These pressures result in a dramatic decrease in cluster density coinciding with an increase in average cluster diameter. The results are similar for Au clusters supported on bare SiO_2 films. By using a mixed TiO_x–SiO_2 thin film containing TiO_x islands instead, though, the effects are much different. Fig. 11 shows images of gold clusters supported on this film before (Fig. 11(a)) and after (Fig. 11(b)) exposure to a 60 Torr CO/O_2 mixture for 2 h at approximately 370 K. As can readily be seen, the cluster density is very similar and there is no noticeable increase in average cluster size.

The histogram of Fig. 12 summarizes the changes in Au cluster density under high temperatures and pressures following nucleation at room temperature for the Ti-free, 8%, and 17% TiO_2–SiO_2 surfaces, respectively. An approximately 70% decrease in Au cluster density is observed on the Ti-free surface due to the thermally induced sintering effect, whereas the extent of sintering of Au clusters is attenuated significantly with an increase in the Ti coverage, with no apparent sintering for the 17% Ti-covered SiO_2 surface. It is apparent from these results that the mixed-oxide surface exhibits sinter resistant properties with respect to thermal treatment and high-pressure gas exposure.

The origin of the observed sinter resistant properties for the titania–silica mixed oxide surface is currently unclear. However, the formation of 2D and/or 3D TiO_x islands are

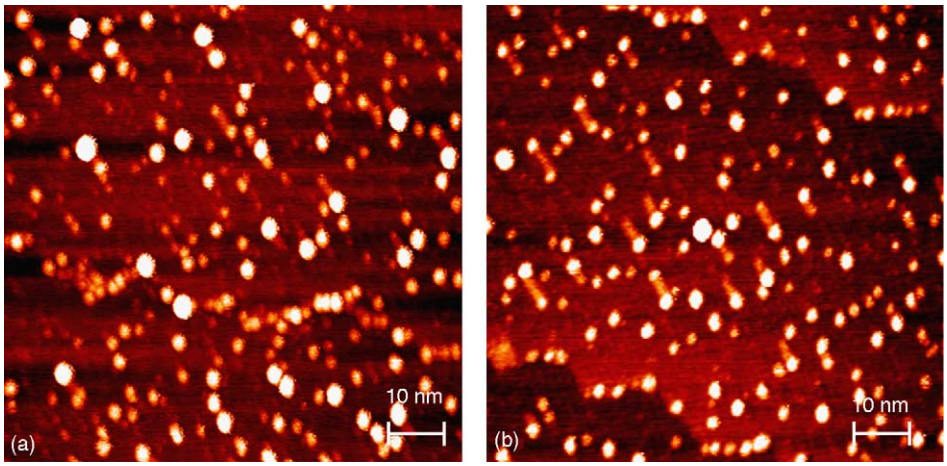

Fig. 9. STM images (100 nm × 100 nm) showing the effects of annealing on Au/TiO_x (17%)–SiO_2: (a) 0.4 ML Au deposited at room temperature; (b) after annealing at 850 K. With the greater amount of Ti comes a greater amount of stability, as the clusters do not sinter under the higher temperatures, maintaining a high number density and the same average size.

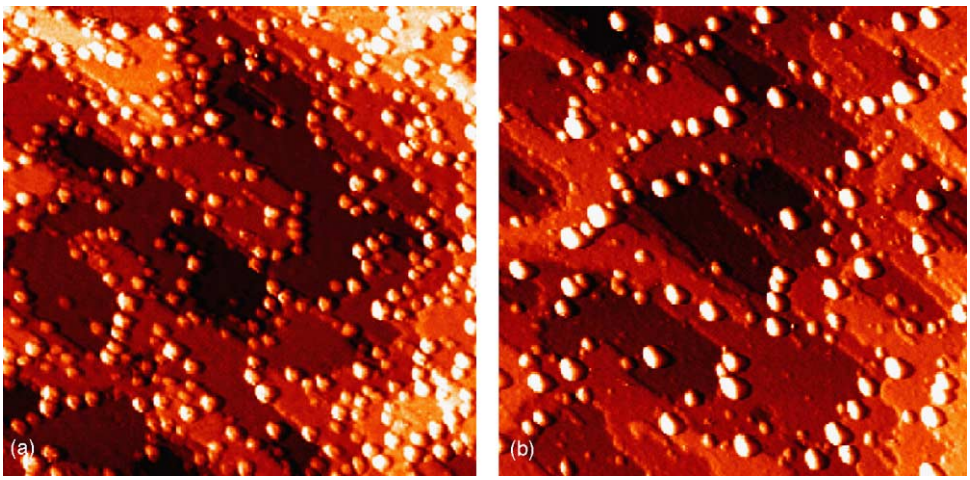

Fig. 10. STM images (100 nm × 100 nm) of Au clusters on TiO_2(1 1 0) showing the effects of reaction pressures on the catalysts: (a) prior to exposure; (b) after exposure to a 10 Torr CO/O_2 mixture.

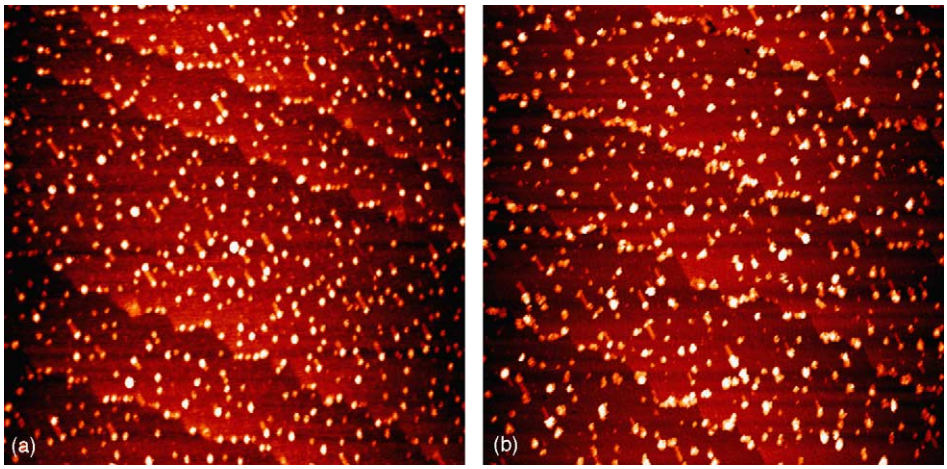

Fig. 11. STM images (200 nm × 200 nm) of Au clusters on TiO_x (17%)–SiO_2 showing the effects of reaction pressures: (a) 0.4 ML Au on TiO_x (17%)–SiO_2 at room temperature; (b) after exposure to a 60 Torr CO/O_2 mixture for 2 h. The cluster number density remains constant, as does the average size.

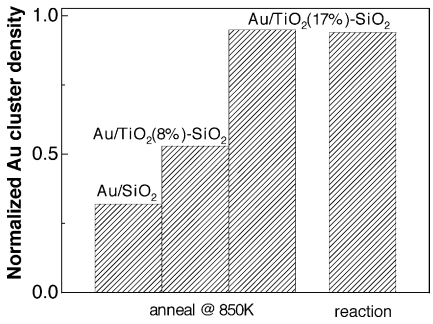

Fig. 12. A histogram showing the effects of annealing samples containing various amounts of Ti. The bar graphs correspond to the cluster number density after annealing divided by the density prior to annealing. The addition of Ti leads to a decrease in cluster sintering. The right hand graph corresponds to the cluster number density after exposing a Au/TiO_x (17%)–SiO_2 sample to a 60 Torr CO/O_2 mixture for 2 h.

possibly important, possibly in physically confining the Au clusters, since silica surfaces with only atomically substituted Ti do not show significantly altered sintering properties. Alternatively, an electronic effect from the TiO_x islands may be the cause of the lack of mobility of the gold clusters. Further investigations are needed and are currently underway in order to better understand the mechanisms leading to the sinter resistant properties of these surfaces.

4. Conclusions

While supported metal clusters are essential to heterogeneous catalysis, many questions remain regarding the effect of cluster size on reactivity and the cluster–support interaction in maintaining cluster stability. In order to better understand these issues, surface science techniques have been applied to “model” catalysts synthesized to mimic commercial catalysts. One of the major thrusts has been the study of the nucleation, growth, and stability of the clusters on various

supports. We have focused on recent studies in our laboratory concerning the interactions between Au and thin SiO_2 and mixed TiO_x–SiO_2 films. These studies have reinforced the importance of surface defects in heterogeneous catalysis, with point defects in the form of Ti-centers showing a large effect on the nucleation and stability of clusters under reaction conditions. A better understanding of these processes gained through the use of model catalysts may very well lead to the development of more efficient and stable nanostructured, technical catalysts.

Acknowledgements

We acknowledge with pleasure the support of this work by U.S. Department of Energy, Office of Basic Energy Science, Division of Chemical Sciences, U.S. Civilian Research & Development Foundation and the Texas Advanced Technology Program under Grant No. 010366-0022-2001.

References

[1] M. Bowker, P. Stone, R. Bennett, N. Perkins, Surf. Sci. 497 (2002) 155–165.
[2] A. Kolmakov, D.W. Goodman, Surf. Sci. 490 (2001) L597–L601.
[3] G. Prevot, O. Meerson, L. Piccolo, C.R. Henry, J. Phys.: Condens. Matter 14 (2002) 4251–4269.
[4] K. Sekizawa, H. Widjaja, S. Maeda, Y. Ozawa, K. Eguchi, Catal. Today 59 (2000) 69–74.
[5] S.K. Shaikhutdinov, R. Meyer, M. Naschitzki, M. Baumer, H.-J. Freund, Catal. Lett. 86 (2003) 211–219.
[6] S.K. Shaikhutdinov, R. Meyer, D. Lahav, M. Baumer, T. Kluner, H.-J. Freund, Phys. Rev. Lett. 91 (2003) 076102.
[7] S.J. Tauster, S.C. Fung, R.L. Garten, J. Am. Chem. Soc. 100 (1978) 170–175.
[8] M. Valden, S. Pak, X. Lai, D.W. Goodman, Catal. Lett. 56 (1998) 7–10.
[9] C. Xu, W.S. Oh, G. Liu, D.Y. Kim, D.W. Goodman, J. Vac. Sci. Technol. A 15 (1997) 1261–1268.
[10] X. Lai, D.W. Goodman, J. Mol. Catal. A 162 (2000) 33–50.
[11] A.F. Carlsson, M. Naschitzki, M. Baumer, H.-J. Freund, J. Phys. Chem. B 107 (2003) 778–785.
[12] D.W. Goodman, Annu. Rev. Phys. Chem. 37 (1986) 425–457.
[13] D.W. Goodman, J. Phys. Chem. 100 (1996) 13090–13102.
[14] S.C. Street, C. Xu, D.W. Goodman, Annu. Rev. Phys. Chem. 48 (1997) 43–68.
[15] C.R. Arumainayagam, C.E. Tripa, J. Xu, J.J.T. Yates, Surf. Sci. 360 (1996) 121–127.
[16] J.J.T. Yates, J. Vac, Sci. Technol. A 13 (1995) 1359–1367.
[17] C.E. Tripa, T.S. Zubkov, J.J.T. Yates, M. Mavrikakis, J.K. Norskov, J. Chem. Phys. 111 (1999) 8651–8658.
[18] T. Zubkov, J.G.A. Morgan, J.J.T. Yates, Chem. Phys. Lett. 362 (2002) 181–184.
[19] F.B.d. Mongeot, M. Scherer, B. Gleich, E. Kopatzki, R.J. Behm, Surf. Sci. 411 (1998) 249–262.
[20] A. Kolmakov, J. Stultz, D.W. Goodman, J. Chem. Phys. 113 (2000) 7564–7570.
[21] L.-Q. Wang, K.F. Ferris, P.X. Skiba, A.N. Shultz, D.R. Baer, M.H. Engelhard, Surf. Sci. 440 (1999) 60–68.
[22] C.D. Valentin, G. Pacchioni, S. Abbet, U. Heiz, J. Phys. Chem. B 106 (2002) 7666–7673.
[23] J. Abad, O. Bohme, E. Roman, Surf. Sci. 549 (2004) 134–142.
[24] H. Hakkinen, S. Abbet, A. Sanchez, U. Heiz, U. Landman, Angew. Chem. Int. 42 (2003) 1297–1300.
[25] A. Sanchez, S. Abbet, U. Heiz, W.-D. Schneider, H. Hakkinen, R.N. Barnett, U. Landman, J. Phys. Chem. A 103 (1999) 9573–9578.
[26] K. Judai, S. Abbet, A.S. Wörza, A.M. Ferrari, L. Giordano, G. Pacchioni, U. Heiz, J. Mol. Catal. A 199 (2003) 103–113.
[27] A. Bogicevic, D.R. Jennison, Surf. Sci. 515 (2002) L481–L486.
[28] D.R. Jennison, A. Bogicevic, Faraday Discuss. 114 (1999) 45–52.
[29] G. Pacchioni, Chem. Phys. Chem. 4 (2003) 1041–1047.
[30] M. Valden, X. Lai, D.W. Goodman, Science 281 (1998) 1647–1650.
[31] E. Wahlstrom, N. Lopez, R. Schaub, P. Thostrup, A. Ronnau, C. Africh, E. Laegsgaard, J.K. Norskov, F. Besenbacher, Phys. Rev. Lett. 90 (2003) 026101.
[32] B.K. Min, A.K. Santra, D.W. Goodman, J. Vac. Sci. Technol. B 21 (2003) 2319–2323.
[33] M. Bäumer, H.-J. Freund, Prog. Surf. Sci. 61 (1999) 127–198.
[34] M. Bäumer, M. Frank, M. Heemeier, R. Kühnemuth, S. Stempel, H.-J. Freund, Surf. Sci. 454–456 (2000) 957–962.
[35] G. Haas, A. Menck, H. Brune, J.V. Barth, J.A. Venables, K. Kern, Phys. Rev. B 61 (2000) 11105–11108.
[36] S. Wendt, Y.D. Kim, D.W. Goodman, Prog. Surf. Sci. 74 (2003) 141–159.
[37] Y.D. Kim, T. Wei, D.W. Goodman, Langmuir 19 (2003) 354–357.
[38] C.E.J. Mitchell, A. Howard, M. Carney, R.G. Egdell, Surf. Sci. 490 (2001) 196–210.
[39] A. Wiltner, A. Rosenhahn, J. Schneider, C. Becker, P. Pervan, M. Milun, M. Kralj, D. Wandelt, Thin Solid Films 400 (2001) 71–75.
[40] J. Carrey, J.-L. Maurice, F. Petroff, A. Vaures, Surf. Sci. 504 (2002) 75–82.
[41] M. Heemeier, S. Stempel, S.K. Shaikhutdinov, J. Libuda, M. Baumer, R.J. Oldman, S.D. Jackson, H.-J. Freund, Surf. Sci. 523 (2003) 103–110.
[42] C. Becker, K.v. Bergmann, A. Rosenhahn, J. Schneider, K. Wandelt, Surf. Sci. 486 (2001) L443–L448.
[43] X. Lai, T.P.S. Clair, M. Valden, D.W. Goodman, Prog. Surf. Sci. 59 (1998) 25–52.
[44] A.K. Santra, B.K. Min, D.W. Goodman, Surf. Sci. 515 (2002) L475–L479.
[45] T. Schroeder, M. Adelt, B. Richter, M. Naschitzki, M. Baumer, H.-J. Freund, Surf. Rev. Lett. 7 (2000) 7–14.
[46] T. Schroeder, M. Adelt, B. Richter, M. Naschitzki, M. Baumer, H.-J. Freund, Microelect. Reliab. 40 (2000) 841–844.
[47] B.K. Min, A.K. Santra, D.W. Goodman, Catal. Today 85 (2003) 113–124.
[48] T. Schroeder, J.B. Giorgi, M. Bäumer, H.-J. Freund, Phys. Rev. B 66 (2002) 165422.
[49] B.K. Min, W.T. Wallace, D.W. Goodman, J. Phys. Chem. B 108 (2004) 14609–14615.
[50] X. Gao, I.E. Wachs, Catal. Today 51 (1999) 233–254.
[51] B.K. Min, W.T. Wallace, A.K. Santra, D.W. Goodman, J. Phys. Chem. B 108 (2004) 16339–16343.
[52] M.S. Chen, A.K. Santra, D.W. Goodman, Phys. Rev. B 69 (2004) 155404.
[53] S.J. Tauster, S.C. Fung, R.T.K. Baker, J.A. Horsley, Science 211 (1981) 1121–1125.